

## Crystal chemistry of the ${}^2_0[M_2^{3+}\phi_2(TO_4)_2]$ sheet: structural principles and crystal structures of ruizite, macfallite and orientite

PAUL B. MOORE, JINCHUAN SHEN<sup>1</sup> AND TAKAHARU ARAKI<sup>2</sup>

Department of the Geophysical Sciences  
The University of Chicago  
Chicago, Illinois 60637

### Abstract

The crystal structures of ruizite,  $Ca_2Mn_3^{3+}(OH)_2[Si_4O_{11}(OH)_2] \cdot 2H_2O$ , monoclinic,  $a = 9.064$ ,  $b = 6.171$ ,  $c = 11.976\text{\AA}$ ,  $\beta = 91.38^\circ$ , space group  $C2/m$ ,  $Z = 2$ ,  $R = 0.084$  for 1546 independent  $F_o$ ; macfallite,  $Ca_2Mn_3^{3+}(OH)_3[SiO_4Si_2O_7]$ , monoclinic,  $a = 10.235$ ,  $b = 6.086$ ,  $c = 8.970\text{\AA}$ ,  $\beta = 110.75^\circ$ , space group  $P2_1/m$ ,  $Z = 2$ ,  $R = 0.184$  for 2437 independent  $F_o$ ; and orientite,  $Ca_2Mn^{2+}Mn_3^{3+}(OH)_4[Si_3O_{10}]$ , orthorhombic,  $a = 9.074$ ,  $b = 19.130$ ,  $c = 6.121\text{\AA}$ , space group  $Bbmm$ ,  $Z = 4$ ,  $R = 0.156$  for 1238 independent  $F_o$ , have been approximately determined. Structure disorder (domains, intergrowths) and/or solid solution probably affect these structures; and true single crystals of these and related compounds are very infrequently encountered.

Ruizite, macfallite, orientite, lawsonite, sursassite, ardenite, pumpellyite, santafeite and bermanite all are based on the same fundamental building block, a sheet  ${}^2_0[M_2^{3+}\square\phi_2(TO_4)_2]$ ,  $\phi$  = anion not associated with a tetrahedron,  $\square$  = vacancy. This sheet is based on a layer of the spinel structure projected down [111] giving the  ${}^2_0[M_3^{3+}\phi_2(TO_4)_2]$  sheet with maximal two-sided plane group symmetry  $[p\bar{3}m1]$ , as found in chloritoid. Ordered vacancies lead to the fundamental building block in this study with plane symmetry  $[c2/m]$ .

Alternatively, the chain component of the fundamental building block (f.b.b.) is  ${}^1_0[M_2^{3+}(O_T)_6(\phi)_2]$  where  $\phi$  usually is  $OH^-$ . A variety of interchain tetrahedral polymers can occur and many explain the disorder in these structures.

### Introduction

Although many of the mineral crystal structures are presently known, the principles behind them are rarely applied, and a holistic structural genealogy is woefully lacking. Much of the inability to evolve a structural genealogy stems from the difficulty of applying graphical enumeration to these problems, and the problem of choice: just which part of the structure should be emphasized? We choose to demonstrate that a fragment—in this case a two-sided slab—is common to several crystal structures of minerals, and may afford a unifying genealogy among these compounds. The list is by no means exhaustive: the compounds selected were those with reasonably refined crystal structure parameters. Briefly, the compounds occur in regimes of low to intermediate temperature, and low to high (cf. lawsonite) pressure.

### Structural principle

The underlying principle is a two-sided plane, a section of the familiar arrangement of spinel,  $Al_2(MgO_4)$ , normal to [111]. In our model, the symbol M refers to cationic species in octahedral coordination (in this case  $Al^{3+}$ ) and T refers to the cationic species in tetrahedral coordination (in this case  $Mg^{2+}$ ). For spinel,  $a = 8.1\text{\AA}$ , this arrangement has  $t_1 = \frac{1}{2}\sqrt{2}a = 5.7\text{\AA}$  and  $t_2 = \sqrt{3}t_1 = 9.9\text{\AA}$ . It is an orthogonal cell and has been extensively exploited for structures derived from spinel by selective site orderings. This arrangement is a sheet with composition  ${}^2_0[M_3O_2(TO_4)_2]$ , maximal point symmetry  $\{\bar{3}2/m\}$  with two-sided plane group  $p\bar{3}2/m$ . The nearest orthohexagonal monoclinic subgroup of this would have point symmetry  $\{2/m\}$  and two-sided plane group  $c2/m$ .

Table 1 outlines the crystal chemical characters of these  $6 \times 9\text{\AA}$  sheet structures, called such because their axial translations approximate these integers. Of the ten representative structure types, only the structure of santafeite is unknown. It is inferred to belong to this group and an approximate formula is given. Earlier, we attempted to solve its structure but it appears to be twinned, in

<sup>1</sup> X-ray Laboratory, Graduate School, Wuhan College of Geology, Beijing, China.

<sup>2</sup> Department of the Geological Sciences, University of Illinois, Chicago, Illinois 60680.

Table 1. Crystal-chemical characters of the  $6 \times 9 \text{ \AA}$  sheet structures<sup>†</sup>

Species	Z	Formula	<u>a</u> ( $\text{\AA}$ )	<u>b</u> ( $\text{\AA}$ )	<u>c</u> ( $\text{\AA}$ )	$\beta$	Space Group	$t_2/t_1$	Two-sided plane	Reference
<b><math>M_3\phi_2(TO_4)_2</math></b>										
Chloritoid	4	$Fe(II)_2Al(OH)_4[Al_3O_2(SiO_4)_2]$	<u>9.52</u>	<u>5.47</u>	18.19	101.57°	C2/c	1.740		1
Theoretical	-	$[M_3\phi_2(TO_4)_2]$ , spinel $a_0 = 8.1 \text{ \AA}$	$t_1 = 5.73$	$t_2 = \sqrt{3}t_1 = 9.92$	---	---	$[P\bar{3}m1, C2/m]$	1.732	$p\bar{3}m1, c2/m$	
<b><math>M_2\phi_2(TO_4)_2</math></b>										
Lawsonite	4	$Ca[Al_2(OH)_2(Si_2O_7)] \cdot H_2O$	<u>5.80</u>	<u>8.83</u>	13.20	---	Cmcm	1.522	c2/m	2
Sursassite	2	$Mn(II)_2[Al_3(OH)_3(SiO_4)(Si_2O_7)]$	<u>8.70</u>	<u>5.79</u>	9.78	108.87	P2/m	1.503	p2/m	3
Ardennite	2	$Mn(II)_2Mg_2(OH)_2[Al_4(OH)_4(AsO_4)(SiO_4)_2(Si_3O_{10})]$	<u>8.71</u>	<u>5.81</u>	18.52	---	Pnmm	1.499	p2/m	4
Pumpellyite	4	$Ca_2Mg[Al_2(OH)_2(SiO_4)(Si_2O_7)]$	<u>8.81</u>	<u>5.94</u>	19.14	97.60	A2/m	1.483	p2/m	5
Orientite	4	$Ca_2(H_2O)_2[Mn(III)_2(OH)_2(Si_3O_{10})]$	<u>9.07</u>	<u>6.12</u>	19.13	---	Bbmm	1.482	b2/m	6
Macfallite	2	$Ca_2[Mn(III)_3(OH)_3(SiO_4)(Si_2O_7)]$	<u>10.23</u>	<u>6.09</u>	<u>8.97</u>	110.75	P2 <sub>1</sub> /m	1.473	p2/m	6
Ruizite	2	$Ca_2[Mn(III)_2(OH)_2(Si_4O_{12}(OH)_2)] \cdot 2H_2O$	<u>9.06</u>	<u>6.17</u>	11.98	91.38	C2/m	1.468	c2/m	6
Santafite	4	$\alpha. Na_3Ca(OH)_2[Mn(III)_3(OH)_3(VO_4)_3] \cdot H_2O$	<u>9.25</u>	<u>6.33</u>	30.00	---	C222 <sub>1</sub> (pseudo ?)	1.461	c2	7
Bermanite	4	$Mn(II)(H_2O)_4[Mn(III)_2(OH)_2(PO_4)_2]$	<u>6.22</u>	<u>8.93</u>	19.25	---	C222 <sub>1</sub> (pseudo)	1.436	c2	8

<sup>†</sup>Species are arranged according to decreasing  $t_2/t_1$  ratio. Cell edges of the f-b-b' are underlined. The space groups of bermanite and possibly santafite are the twinned groups. The two-sided plane refers to the f-b-b' in the structures.

<sup>1</sup>Harrison and Brindley (1957). <sup>2</sup>Rumanova and Skiptrova (1959). <sup>3</sup>Mellini and Merlino (1982). <sup>4</sup>Donnay and Allmann (1968). <sup>5</sup>Gottardi (1965).

<sup>6</sup>This study. <sup>7</sup>Sun and Weber (1958), with b and c axes interchanged.

<sup>8</sup>Kampf and Moore (1976), after transformation a = [101], b = [10 $\bar{1}$ ], c = [010]. Note  $\beta^* = 90.25^\circ$ .

much the same fashion as bermanite. The actual space group of bermanite is  $P2_1$ , but twinning usually leads to the  $C222_1$  space group (Kampf and Moore, 1976). Ruizite, formerly proposed as  $P2_1/c$  by Williams and Duggan (1977), is  $C2/m$  for our crystal from Kuruman, South Africa. The "theoretical" structure, which is included in the  $M_3\phi_2(TO_4)_2$  ( $\phi$  = arbitrary symbol for an anion) subgrouping, would be a slab of the spinel structure normal to the [111] direction. The space group  $P\bar{3}m1$  for this two-sided plane includes the orthogonal component of  $C2/m$  as a subgroup. The sheet of cubic close-packing is the basis for the ratio  $t_2/t_1 = \sqrt{3}/1 = 1.732$ .

An outline of the  $P\bar{3}m1$ ,  $a_1 = 6 \text{ \AA}$ , arrangement is presented in Figure 1. This sheet consists of rows of populated octahedra alternating with rows of insular octahedra and the tetrahedra. Chloritoid actually possesses this slab as the  $[Al_3O_2(SiO_4)_2]$  unit and distortions lead to monoclinic or triclinic symmetry, but the  $t_2/t_1$  ratio is close to  $\sqrt{3}$ . If rows of populated octahedra alternate with rows of octahedral voids and the tetrahedra, then the formula  $M_2\phi_2(TO_4)_2$  obtains, where  $\square$  is a vacancy. This arrangement is an ordered subgroup of  $P\bar{3}m1$ . Its maximal space group is  $C2/m$ . The most pronounced distortion in these structures arises from cation-cation repulsion effects across the shared edges and a subsequent diminution in the  $t_2/t_1$  ratio. If  $a = 9 \text{ \AA}$  and  $b = 6 \text{ \AA}$ , then  $t_2/t_1 = 1.50$ , close to the average 1.482 for the nine structure types of  $M_2\phi_2(TO_4)_2$ . The range is 1.545 to 1.428 for these compounds. No attempt was made to transform the cell criteria in Table 1. Rather, the  $6 \times 9 \text{ \AA}$  axes were underlined and the ratio was derived directly from knowledge of the structure and orientation of the octahedral chains. All the structures approximate the  $6 \times 9$  module, and division or multiplication of these axial

repeats was not required. This adds some credence to the  $M_2\phi_2(TO_4)_2$  unit as a fundamental building block. The direction normal to this sheet is the basis of a variety of tetrahedral polymerizations, as we shall see.

Figure 2a is a construction of the idealized  $C2/m$  sheet showing the important symmetry operations. Note that all populated octahedra are based on the unit  $M(O_T)_4(\phi)_2$ , where  $\phi$  are in *trans* arrangement with respect to the

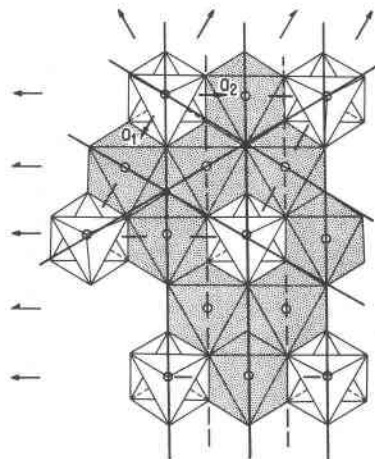


Fig. 1. Sheet of  ${}^2_2[M_3\phi_2(TO_4)_2]$  showing some of the symmetry elements in space group  $P\bar{3}m1$  and the unit cell outline with  $a_1, a_2 \sim 6 \text{ \AA}$ . Some symmetry elements  $m, \bar{1}, 2, 2_1$  and axial glides are shown and are slightly offset to ease visualization of the sheet.

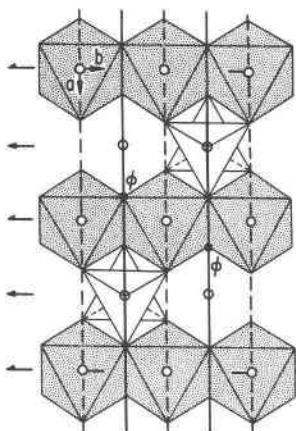
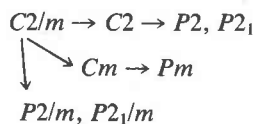


Fig. 2a. Sheet of  ${}^2_2[M_2\Box\phi_2(TO_4)_2]$  showing  $m$ ,  $\bar{1}(1)$ ,  $\bar{1}(2)$ ,  $2$ ,  $2_1$  and  $a$ -axial glides in space group  $C2/m$ , the ordered subgroup of  $P\bar{3}m1$ . This is the fundamental building block for the structures in the text. The axes are approximately  $a = 9\text{\AA}$ ,  $b = 6\text{\AA}$ .

octahedral center. Monoclinic same-cell subgroups of this space group include



Often, it is more convenient to project the structure down the shortest axis, frequently an axis of symmetry. Representation of the sheet down this direction is featured in Figure 2b. Since the axis of projection is the  $6\text{\AA}$  direction, it coincides with the direction of octahedral edge-sharing chains. It corresponds to the  $[110]$  direction of the spinel structure.

The  $trans\text{-}M(O_T)_4(\phi)_2$  immediately presents a problem. Is  $cis\text{-}M(O_T)_4(\phi)_2$  possible? Figure 3 shows such an arrangement with  $a' = a/2$ ,  $b' = b$ , maximal space group  $P2/m$ . Of the eight known structures in Table 1, all involve  $trans\text{-}M(O_T)_4(\phi)_2$  and the  $cis\text{-}M(O_T)_4(\phi)_2$  arrangement has yet to be found. It is believed that the pronounced Jahn-Teller axial distortion from the  $d_{z^2}$  molecu-

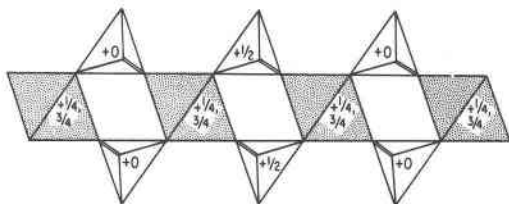


Fig. 2b. Alternative projection of  ${}^2_2[M_2\Box\phi_2(TO_4)_2]$ , a frequent projection for the Fig. 5 series. The edge-sharing  ${}^1_2M\phi O_{T_3}$   $6\text{\AA}$  octahedral chains are normal to the paper. The  $9\text{\AA}$  direction runs from left to right and the intersheet portion runs from north to south. Heights are given as fractional coordinates of the  $6\text{\AA}$  direction.

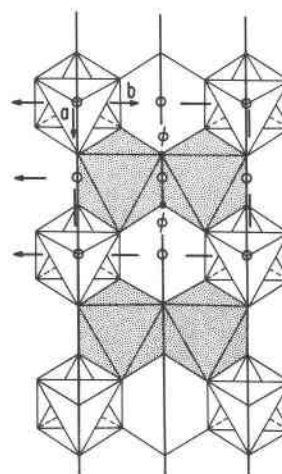


Fig. 3. The hypothetical structure built of  $cis\text{-}M\phi_2O_{T_4}$  octahedra. The symmetry elements  $m$ ,  $\bar{1}$  are shown and the space group is  $P2/m$ . The axes are approximately  $a = 4.5\text{\AA}$  and  $b = 6\text{\AA}$ .

lar orbital for  $d^4Mn^{3+}$  in high spin configuration forces the  $trans$  arrangement, but this does not rule out the  $cis$  arrangement for some isotropic cation, say  $Al^{3+}$ .

In every structure involving  $Mn^{3+}$  (orientite, macfallite, ruizite, bermanite), a common feature of polyhedral distortion appears: the polyhedron is elongate with  $4Mn^{3+}\text{-O}$  *ca.*  $1.93\text{\AA}$  and  $2Mn^{3+}\text{-O}$  *ca.*  $2.21\text{\AA}$ , with  ${}^{16}Mn^{3+}\text{-O} = 2.02\text{\AA}$  average (Table 2). The major component of the elongate bonds is oriented parallel to the  $6\text{\AA}$  axis, the direction which is normal to the octahedral shared edges in the  ${}^1_2[Mn^{3+}\phi_4]$  octahedral chain. Isolating the sheet of octahedra and tetrahedra in Figure 2, three kinds of ligand arrangements occur. The first is (a)  $2Mn^{3+} + 1Si^{4+}$  and is an  $O^{2-}$  ligand. The second is (b)  $1Mn^{3+} + 1Si^{4+}$ , also an  $O^{2-}$  ligand. The third is (c)  $2Mn^{3+}$ , corresponding to the hydroxyl ( $OH^-$ ) ligand. In each structure, the elongate  $Mn^{3+}\text{-O}$  bonds correspond to the ligand at (a). The combination of the direction of cation-cation repulsion and the orientation of the elongate verti-

Table 2. Meridional and apical  $Mn^{3+}\text{-O}$  bonds for the fundamental building block in bermanite, orientite, ruizite and macfallite<sup>†</sup>

	Meridional bonds				Apical bonds		Average
Bermanite							
Mn(1)	1.89	1.91	1.95	1.96	2.20	2.20	2.02 Å
Mn(2)	1.89	1.91	1.94	1.95	2.21	2.24	2.02
Orientite							
Mn(1)	1.91	1.91	1.96	1.96	2.20	2.20	2.02
Ruizite							
Mn	1.91	1.91	1.95	1.95	2.20	2.20	2.02
Macfallite							
Mn(3)	1.94	1.94	1.94	1.94	2.22	2.22	2.03
Grand average	1.93 Å				2.21 Å		2.02 Å
Range	1.89-1.96 Å				2.20-2.24 Å		

<sup>†</sup>Mn(1) in macfallite excluded because it contains significant aluminum. The bermanite data are from Kampf and Moore (1976).

ces result in a  $t_2/t_1$  ratio that is relatively small. Indeed, all five structure types with the  $[\text{Mn}^{3+}(\text{OH})_2(\text{TO}_4)_2]$  building block possess the smallest ratios among the compounds in Table 1.

The  $[\text{Mn}^{3+}(\text{OH})_2(\text{TO}_4)_2]$  fundamental building block (abbreviated f.b.b.) imprints other portions of the structure as well, even though linking units of varying dimensions occur between the sheets. The fundamental building block is a portion of a crystal structure which also is an invariant component of several non-equivalent crystal structures. In the structures of ruizite, orientite, macfallite, pumpellyite and ardennite larger cations such as  $\text{Mn}^{2+}$  and  $\text{Ca}^{2+}$  occur in seven-fold coordination by anions and the polyhedron corresponds to No. 23 with maximal point symmetry  $C_{2v}$  ( $mm2$ ) in Britton and Dunitz (1973). The polyhedron is reminiscent of the gable disphenoid of order 8 which occurs as the coordination polyhedron about  $\text{Ca}^{2+}$  and  $\text{Na}^{1+}$  in several structures (Moore, 1981). The gable disphenoid is constructed by rotating one square face  $90^\circ$  relative to the other of two equilateral trigonal prisms and fusing them together. Polyhedron No. 23 is obtained by fusing an equilateral trigonal prism and a square pyramid together at the square face, or can be simply called the monocapped trigonal prism. In every case, three vertices of a trigonal prismatic component link to vertices between successive octahedra in the  $6\text{Å}$  chain. These vertices are of the type  $a(\times 1)$  and  $b(\times 2)$ . The remaining four vertices exhibit a variety of coordinations since they are the regions away from the f.b.b. Other coordinating cations to these vertices can be  $\text{Si}^{4+}$ ,  $2\text{Si}^{4+}$ ,  $\text{As}^{5+}$ ,  $\text{M}^{2+}$ ,  $\text{M}^{3+}$ —or the vertices can be other ligands such as  $(\text{OH}^-)$  and  $(\text{H}_2\text{O})$ .

Lawsonite possesses the same f.b.b. and the interleaving  $\text{Ca}^{2+}$  has related but distinct coordination, being of

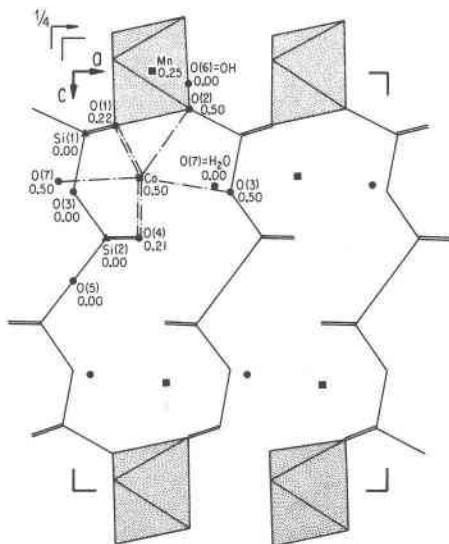


Fig. 5a. Representation of the ruizite structure down the [010] direction. Atoms labelled correspond to Table 5a.

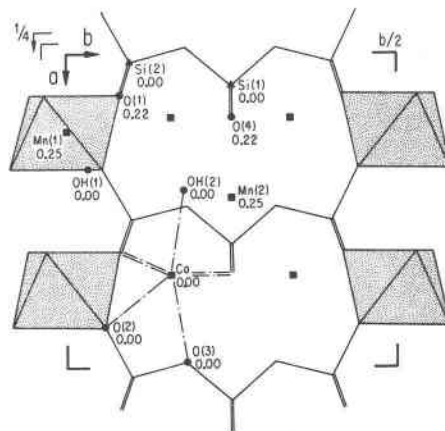


Fig. 5c. Representation of the disordered orientite structure down [001]. Note  $[\text{Si}_3\text{O}_{10}]$  groups and disordered Mn(2) are drawn in.

number 6. The coordination on the square pyramidal side is the same, but on the trigonal side the two oxygens are replaced by one, resulting in a distorted octahedron. The trigonal oxygens O(3) in Figure 4, which represents lawsonite, are present but their distances are too long for nearest neighbor coordination. Bermanite, which has intersheet  $\text{Mn}^{2+}(\text{H}_2\text{O})_4(\text{Op})_2$ , bridges the f.b.b.'s by the (Op) oxygens.

The  $X\phi_7$  polyhedra commonly polymerize to each other through edge-sharing. In ruizite they are isolated, but they occur as edge dimers in ardennite and orientite, where  $\text{Ca}-\text{O}$  of the terminal square planar bonds are parallel, and in pumpellyite and macfallite where they are opposed. Portions of these structures are featured in the Figure 5 series.

The tetrahedral links between the f.b.b.'s are interesting. The bases of the tetrahedral segments such as  $\text{O}(1)-\text{O}(2)-\text{O}(1)$  in orientite (Fig. 6c) link to the f.b.b. of the same structure (Fig. 5c). The tetrahedral units are homologues of the linear sorosilicate series  $[\text{T}_n\text{O}_{3n+1}]$ , where  $n$

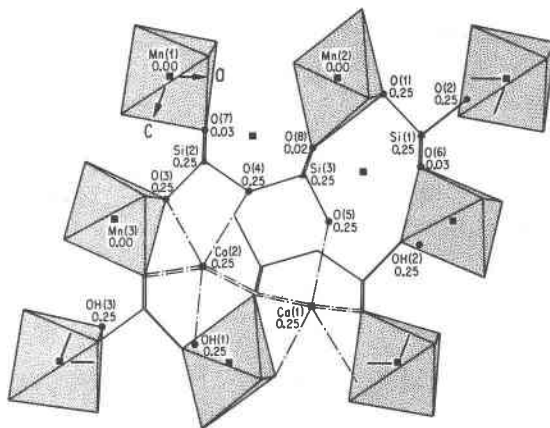


Fig. 5e. Representation of the macfallite structure down [010].

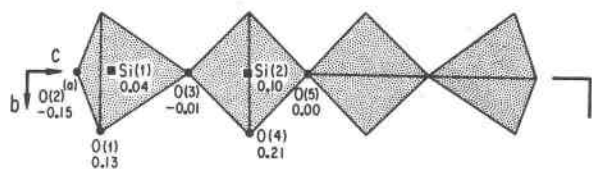


Fig. 6a. Tetrahedral interlayer link in ruizite down [100].

= 1,  $\text{Si}\phi_4$ ; 2,  $\text{Si}_2\phi_7$ ; 3,  $\text{Si}_3\phi_{10}$ ; and 4,  $\text{Si}_4\phi_{13}$ . Representatives include bermanite and possibly santafeite ( $n = 1$ ); lawsonite ( $n = 2$ ); pumpellyite, macfallite, sursassite ( $n = 1, 2$ ); orientite ( $n = 3$ ); ardenite ( $n = 1, 3$ ); ruizite ( $n = 4$ ). In the Figure 6 series, the tetrahedral units were projected down the  $9\text{\AA}$  axis and their dispositions approximate the tetrahedral arrangement in the rocksalt structure down [100]. For example, the central tetrahedra in ruizite are viewed down the approximate 2-fold rotors implicit in the  $\bar{4}$  symmetry; the entire  $\text{Si}_4\phi_{13}$  unit (Fig. 6a) can be considered as the fusion of the  $[\text{Si}_2\text{O}_7]$  dimers in pumpellyite, sursassite and macfallite at the inversion center. This point of fusion forces a central Si–O–Si =  $180^\circ$  angle in ruizite.

The structures thus can be conceived as sheets of the  $\infty[\text{M}_2\phi_2(\text{TO}_4)_2]$  fundamental building block with connected  $(\text{Ca}, \text{Mn}^{2+})\phi_7$  polyhedra No. 23. In turn, these sheets are connected to symmetry-translated sheets by a variety of (silicate) polymers, including  $(\text{Mn}^{2+}(\text{H}_2\text{O})_4)$  in bermanite;  $[\text{Si}_2\text{O}_7]$  in lawsonite;  $[\text{SiO}_4] + [\text{Si}_2\text{O}_7]$  in sursassite, pumpellyite, macfallite;  $[\text{Si}_3\text{O}_{10}]$  in orientite;  $[\text{AsO}_4] + [\text{SiO}_4] + [\text{Si}_3\text{O}_{10}]$  in ardenite; and  $[\text{Si}_4\text{O}_{11}(\text{OH})_2]$  in ruizite. Naturally, portions of these polymers are also components of the fundamental building blocks. For example, ruizite could be rewritten  $[\text{Ca}_2(\text{H}_2\text{O})_2\text{Si}_2\text{O}_3(\text{OH})_2][\text{Mn}_2^{3+}(\text{OH})_2(\text{SiO}_4)_2]$  where the first brackets represent the material beyond the border of the fundamental building block denoted in the second brackets. With this spirit in mind, the formulae in Table 1

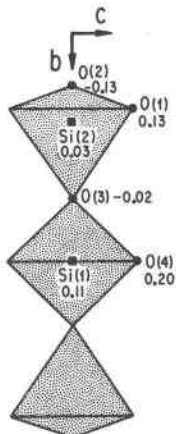


Fig. 6c. Tetrahedral interlayer link in orientite down [100]. Here, the connected  $[\text{Si}_3\text{O}_{10}]$  unit is shown.

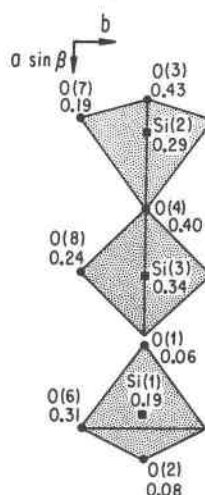


Fig. 6e. Tetrahedral interlayer link in macfallite down [001] showing  $[\text{Si}_2\text{O}_7]$  and  $[\text{SiO}_4]$  units.

have been rewritten in Table 3 to stress two critical regions: the intersheet material in the first bracket and the fundamental sheet or building block in the second bracket. To effect this, the structures in the Figures 5 and 6 series were inspected. The fundamental sheet was isolated and subtracted from the formula in Table 1. What remained was cross-checked on the structure drawings and defined as intersheet material. In only one structure, lawsonite, was partitioning between regions not exact since one extra oxygen had to be added. This was consequently subtracted from the intersheet material.

Some very interesting conclusions can be drawn from Table 3. First, sursassite and macfallite are chemically and structurally related as their recent structure determinations indicate (Mellini and Merlino, 1982; this study), the major difference being pronounced Jahn–Teller distortion in the latter compound. Second, mistakes in the intersheet region should be quite likely among compounds which have the same fundamental building blocks and similar metric relations in these building blocks such

Table 3. Partitioning of formulae in Table 1 into intersheet and fundamental building block<sup>†</sup>

Species	First bracket (Intersheet)	Second bracket (f.b.b.)
Lawsonite	$\text{Ca}(\text{H}_2\text{O})(\text{O})_{-1}$	$\text{Al}_2(\text{OH})_2(\text{SiO}_4)_2$
Sursassite	$\text{Mn}_2^{2+}\text{Al}(\text{OH})\text{SiO}_3$	$\text{Al}_2(\text{OH})_2(\text{SiO}_4)_2$
Ardennite	$\text{Mn}_2^{2+}\text{Mg}_2(\text{OH})_2\text{SiO}_2\text{AsO}_4$	$2\text{Al}_2(\text{OH})_2(\text{SiO}_4)_2$
Pumpellyite	$\text{Ca}_2(\text{H}_2\text{O})\text{MgSiO}_3$	$\text{Al}_2(\text{OH})_2(\text{SiO}_4)_2$
Orientite	$\text{Ca}_2(\text{H}_2\text{O})_2\text{SiO}_2$	$\text{Mn}_2^{3+}(\text{OH})_2(\text{SiO}_4)_2$
MacFallite	$\text{Ca}_2\text{Mn}^{3+}(\text{OH})\text{SiO}_3$	$\text{Mn}_2^{3+}(\text{OH})_2(\text{SiO}_4)_2$
Ruizite	$\text{Ca}_2(\text{H}_2\text{O})_2\text{Si}_2\text{O}_3(\text{OH})_2$	$\text{Mn}_2^{3+}(\text{OH})_2(\text{SiO}_4)_2$
Bermanite	$\text{Mn}^{2+}(\text{H}_2\text{O})_4$	$\text{Mn}_2^{3+}(\text{OH})_2(\text{PO}_4)_2$

<sup>†</sup>Santafeite omitted because structure is not known. Orientite assumes the member without  $\text{Mn}^{2+}$ . Note isomorphism between sursassite and macfallite. Lawsonite has negative oxygen in first bracket to balance charge.

as  $[\text{Mn}_2^{3+}(\text{OH})_2(\text{SiO}_4)_2]$  in orientite, macfallite and ruizite. We offer evidence here that the structures of the crystals used in our study probably represent a substantial degree of domain disorder, since despite structure solution and convergence, their final reliability factors were not of satisfactory quality.

### Experimental

The experimental details of ruizite, macfallite and orientite are summarized in Table 4. Crystals of ruizite from the type locality at Christmas Mine, Gila County, Arizona, were kindly provided by Dr. Sidney A. Williams. Unfortunately, they were unsuitable for data collection because of twinning and very small crystal size. Shortly thereafter, Mr. John S. White, Jr., of the U.S. National Museum (Smithsonian Institution) kindly sent sharp brown prismatic crystals from the N'Chwaning Mine, Kuruman,

Cape Province, South Africa (USNM No. 136812), and these were used throughout the remainder of the study. Good agreement appears in the unit cell parameters compared with the original study by Williams and Duggan (1977), but we do not agree on the space group. Since  $P2_1/c$  is not a same-cell subgroup of  $C2/m$ , caution must be exerted without additional study on the type material, since it is possible (though unlikely) that two closely related species are involved.

Macfallite and orientite samples both were collected by the senior author on the dumps of the type locality for the former mineral, near Lake Manganese, Copper Harbor, Keweenaw County, Michigan. Great effort was expended to obtain adequate crystals, since the minerals are usually twinned and occur with splayed surfaces. The crystals finally selected were deep maroon and transparent. The end-member formulae in Table 4 for these minerals lead to a calculated density higher than observed, due to the presence of  $\text{Al}^{3+}$  in these crystals (Moore et al., 1979). For

Table 4. Ruizite, macfallite and orientite: experimental details

(A) Crystal Cell Data			
	Ruizite	MacFallite	Orientite
a, Å	9.064(1)	10.235(3)	9.074(4)
b, Å	6.171(2)	6.086(6)	19.130(7)
c, Å	11.976(3)	8.970(5)	6.121(5)
$\beta$ , deg	91.38(2)	110.75(3)	-
Space group	$C2/m$	$P2_1/m$	Bbmm
Z	2	2	4
Formula	$\text{Ca}_2\text{Mn}_2\text{Si}_{4.011}(\text{OH})_4 \cdot 2\text{H}_2\text{O}$	$\text{Ca}_2\text{Mn}_3\text{Si}_{3.011}(\text{OH})_3$	$\text{Ca}_2\text{Mn}_3\text{Si}_{3.010}(\text{OH})_4$
$\rho(\text{calc})$ , $\text{g cm}^{-3}$	2.89	3.53	3.48
Specific gravity*	2.9	3.43	3.33
$\mu$ , $\text{cm}^{-1}$	31.7	50.9	50.1

(B) Intensity Measurements			
Crystal size, mm ( $l_1a$ , $l_1b$ , $l_1c$ )	0.30, 0.15, 0.12	0.15, 0.30, 0.10	0.12, 0.15, 0.12
Max $(\sin \theta)/\lambda$	0.72	0.70	0.70
Scan speed (deg per min)	2.0	2.0	2.0
Background counts	-----Stationary, 20s at beginning and end of scan-----		
Radiation	----- $\text{MoK}_\alpha$ ( $\lambda$ 0.70926 Å), graphite monochromator-----		
Independent $F_0$	1546	2437	1238
Diffractometer	-----PICKER FACS-1-----		

(C) Refinement of the Structure			
$R = \sum  F_0  -  F_C  / \sum  F_0 $	0.084	0.184	0.156
$R_w = \{ \sum_w ( F_0  -  F_C )^2 / \sum_w F_0^2 \}^{1/2}$ , $w = \sigma^{-2}(F_0)$	0.095	0.140	0.143
Scale factor	1.441(6)	4.37(3)	1.14(1)
Variable parameters	72	123	69

\*Ruizite, Williams and Duggan (1977); macfallite and orientite, Moore et al. (1979) who discuss significant  $\text{Al}^{3+}$  in these compounds.



Table 7b. Macfallite: bond distances and angles<sup>†</sup>

Mn(1)			Mn(2)			Mn(3)		
2 Mn(1)-O(7)	1.91 Å		2 Mn(2)-OH(1)	1.91		2 Mn(3)-OH(2)	1.94	
2 -OH(3)	1.98		2 -O(1)	2.11		2 -O(6)	1.94	
2 -O(2)	2.06		2 -O(8)	2.18		2 -O(3)	2.21	
average	1.97		average	2.07		average	2.03	
		angle (deg.)						
*2 O(2)-OH(3)	2.64	81.5	*2 O(1)-OH(1)	2.61	80.8	2 O(6)-OH(2)	2.69	88.0
2 O(7)-OH(3)	2.73	89.2	2 O(8)-OH(1) <sup>(1)</sup>	2.88	89.4	*2 O(3)-OH(2)	2.79	84.1
2 O(7)-OH(3) <sup>(1)</sup>	2.77	90.8	2 O(8)-OH(1)	2.91	90.6	2 O(6)-OH(2) <sup>(1)</sup>	2.79	92.0
2 O(2)-O(7) <sup>(1)</sup>	2.79	89.3	2 O(1)-O(8)	2.99	88.6	2 O(3)-O(6) <sup>(1)</sup>	2.86	86.6
2 O(2)-O(7)	2.82	90.7	2 O(1)-OH(1) <sup>(1)</sup>	3.06	99.2	2 O(3)-O(6)	3.03	93.4
2 O(2)-OH(3) <sup>(1)</sup>	3.06	98.5	2 O(1)-O(8) <sup>(1)</sup>	3.07	91.4	2 O(3)-OH(2) <sup>(1)</sup>	3.09	95.9
average	2.80	90.0	average	2.92	90.0	average	2.88	90.0
Si(1)			Si(2)			Si(3)		
1 Si(1)-O(2)	1.62		2 Si(2)-O(7)	1.62		2 Si(3)-O(8)	1.63	
2 -O(6)	1.64		1 -O(3)	1.63		1 -O(5)	1.66	
1 -O(1)	1.65		1 -O(4)	1.65		1 -O(4)	1.69	
average	1.64		average	1.63		average	1.65	
1 O(1)-O(2)	2.52	101.1	1 O(3)-O(4)	2.58	103.5	1 O(4)-O(5)	2.63	103.5
1 O(6)-O(6) <sup>(2)</sup>	2.64	107.2	2 O(4)-O(7)	2.63	106.9	2 O(5)-O(8)	2.68	109.3
2 O(2)-O(6)	2.71	112.6	1 O(7)-O(7) <sup>(2)</sup>	2.70	112.7	2 O(4)-O(8)	2.69	108.3
2 O(1)-O(6)	2.72	111.7	2 O(3)-O(7)	2.71	113.0	1 O(8)-O(8) <sup>(2)</sup>	2.78	117.3
average	2.67	109.5	average	2.66	109.3	average	2.69	109.3
Ca(1)			Ca(2)					
2 Ca(1)-O(7) <sup>(1)</sup>	2.29		1 Ca(2)-OH(1)	2.28				
2 -O(8) <sup>(1)</sup>	2.43		1 -O(3)	2.34				
1 -O(1)	2.46		2 -O(6) <sup>(1)</sup>	2.38				
1 -O(5)	2.46		2 -O(8) <sup>(1)</sup>	2.43				
1 -O(2)	2.74		1 -O(4)	2.66				
average	2.44		average	2.41				

<sup>†</sup> Estimated standard errors are within 0.04 Å for O-O<sup>-</sup> and Ca-O; 0.03 Å for Mn-O and Si-O; 0.9° for angles. The equivalent positions (referred to Table 5b) are designated as superscripts and are (1) = -x, -y, -z; (2) = x, ½-y, z; (3) = -x, ½+y, -z.

\* Mn<sup>3+</sup>-Mn<sup>3+</sup> shared edges.

the structure factors.<sup>3</sup> It should be noted that the anisotropic thermal parameters for these crystals are more likely manifestations of intergrowths and domain disorder, rather than descriptions of true thermal motions.

### Discussion of the structures

All three structures—ruizite, macfallite, and orientite—are based on the [Mn<sup>3+</sup>(OH)<sub>2</sub>(SiO<sub>4</sub>)<sub>2</sub>] fundamental build-

<sup>3</sup> To obtain copies of Tables 6a, 6b, 6c, 8, and Figures 4, 5b, 5d, 6b, 6d and 6f, order Document AM-85-261 from the Business Office, Mineralogical Society of America, 2000 Florida Avenue, N.W., Washington, D. C. 20009. Please remit \$5.00 in advance for the microfiche.

ing block. They differ in the nature of the intersheet material. The bond distance averages for Mn<sup>3+</sup>-O in the f.b.b. are Mn-O = 2.02 for ruizite, Mn(1)-O = 1.97 and Mn(3)-O = 2.03 for macfallite and Mn(1)-O = 2.02 Å for orientite. The Mn(1)-O distance in macfallite is unusually short, but this is evidently the site where substantial Al<sup>3+</sup> is sequestered according to Table 5b. The intersheet larger cations are particularly interesting. The Ca-O averages for seven coordination are Ca-O = 2.46 in ruizite, Ca(1)-O = 2.44 and Ca(2)-O = 2.41 Å in macfallite, and Ca-O = 2.45 Å in orientite. There is no evidence of significant substitution at the Ca sites in these structures. The Ca-O ranges are from about 2.3 to 2.7 Å, and

Table 7c. Orientite: bond distances and angles<sup>†</sup>

Mn(1)			Mn(2)			Si(2)		
2 Mn(1)-O(1)	1.91 Å		2 Mn(2)-O(3) <sup>(a)</sup>	2.04		1 Si(2)-O(2)	1.61	
2 -OH(1)	1.96		2 -OH(2)	2.09		2 -O(1)	1.63	
2 -O(2) <sup>(2a)</sup>	2.20		1 -O(4)	2.27		1 -O(3)	1.66	
average	2.02		1 -O(4) <sup>(2a)</sup>	2.27		average	1.63	
			average	2.13				
		angle (deg.)						
2 OH(1)-O(1)	2.71	89.3	**1 O(3) <sup>(a)</sup> -O(3) <sup>(4a)</sup>	2.65		1 O(2)-O(3)	2.55	102.6
2 OH(1)-O(1) <sup>(1a)</sup>	2.76	91.0	2 O(3) <sup>(a)</sup> -O(4) <sup>(2a)</sup>	2.77		1 O(1)-O(1) <sup>(2)</sup>	2.65	108.7
*2 OH(1)-O(2) <sup>(4)</sup>	2.77	83.4	1 OH(2)-OH(2) <sup>(4)</sup>	2.81		2 O(1)-O(3)	2.67	108.7
2 O(1)-O(2) <sup>(a)</sup>	2.84	87.3	2 O(4)-OH(2)	2.85		2 O(1)-O(2)	2.71	113.9
2 O(1)-O(2) <sup>(1)</sup>	2.98	92.7	2 O(3) <sup>(a)</sup> -OH(2)	3.10		average	2.66	109.4
2 OH(1)-O(2) <sup>(a)</sup>	3.11	96.6	2 O(3) <sup>(a)</sup> -O(4)	3.31				
average	2.86	90.0	2 O(4) <sup>(2a)</sup> -OH(2)	3.31		1 Si(1)-Mn(2) <sup>(a)</sup>	2.05	
			average	3.01		1 Ca-Si(2)	3.24	
Si(1)			Ca					
2 Si(1)-O(4)	1.64		2 Ca-O(1) <sup>(a)</sup>	2.36				
2 -O(3)	1.73		2 -O(4) <sup>(a)</sup>	2.43				
average	1.68		1 -OH(2)	2.43				
			1 -O(2)	2.49				
			1 -O(3)	2.62				
**1 O(3)-O(3) <sup>(3)</sup>	2.65	100.0	average	2.45				
1 O(4)-O(4) <sup>(2)</sup>	2.75	113.5						
4 O(3)-O(4)	2.77	110.7						
average	2.75	109.4						

<sup>†</sup> Estimated standard errors are within 0.04 Å for O-O<sup>-</sup> and Ca-O; 0.03 Å for Mn-O and Si-O; 0.9° for angles. The equivalent positions (referred to Table 5c) are designated as superscripts and are (a) =  $\frac{1}{2}$  0  $\frac{1}{2}$ ; (1) = -x, -y, -z; (2) = x, y, -z; (3) = x,  $\frac{1}{2}$ -y, -z; (4) = x,  $\frac{1}{2}$ -y, z.

\*\*Mn<sup>3+</sup>-Mn<sup>3+</sup> shared edges.    \*\*Mn<sup>2+</sup>-Si<sup>4+</sup> shared edges (disorder).

the Ca $\phi_7$  polyhedron No. 23 appears to be a characteristic feature in this family of structures.

Macfallite and orientite possess additional interlayer Mn(2) in their structures. Their respective averages are Mn(2)-O = 2.07 and 2.13 Å. Both compounds are interpreted as possessing a (Mn<sup>2+</sup>, Mn<sup>3+</sup>) solid solution at this site, but additional Mg<sup>2+</sup> may also play a major role as, for example, in ardenite, which relates to orientite; and sursassite, which is nearly isostructural with macfallite. This implies that a complex coupled relationship may exist between O<sup>2-</sup>, OH<sup>-</sup> and possibly H<sub>2</sub>O among some of the coordinating anions about Mn(2).

In orientite, the Mn(2) site is evidently half-occupied since the Mn(2)-Si(1) = 2.05 Å distance is unusually short. This would suggest that an average of two ordering schemes is being observed. In the first scheme, consider the absence of Mn(2). Then the orientite structure formula would be Ca<sub>2</sub>Mn<sub>2</sub><sup>3+</sup>(OH)<sub>2</sub>(Si<sub>3</sub>O<sub>10</sub>). Here, OH(2) is also eliminated, which would reduce the coordination about

Ca to six. In the second scheme Mn(2) is fully occupied but Si(1) is empty. A charge-balanced example would be Ca<sub>2</sub>Mn<sup>2+</sup>(OH)<sub>2</sub>[Mn<sup>3+</sup>(OH)<sub>2</sub>(SiO<sub>4</sub>)<sub>2</sub>]. Orientite would represent compositions somewhere along the join between these two end-member compositions. Moore et al. (1979) suggested Ca<sub>2</sub>Mn<sup>2+</sup>Mn<sup>3+</sup>(OH)<sub>4</sub>(Si<sub>3</sub>O<sub>10</sub>)-Ca<sub>2</sub>Mn<sup>3+</sup>(OH)<sub>2</sub>(Si<sub>3</sub>O<sub>10</sub>) · 2H<sub>2</sub>O for the series at a time when the structure was not known. Interestingly, Mellini and Merlino (1982) proposed a model where [SiO<sub>4</sub>] tetrahedra alternate with [Si<sub>3</sub>O<sub>10</sub>] tetrahedra across the fundamental building block and this would appear to be the best compromise between the two extremes.

This hypothesis appears to bring several observations into account. The first is the presence of [Si<sub>4</sub>O<sub>11</sub>(OH)<sub>2</sub>] tetramers in ruizite, where on the average two out of four equivalent oxygens are replaced by hydroxyl groups to balance charge. In orientite, two out of four equivalent oxygens likewise appear to be replaced by hydroxyls. The second problem concerns the formula unit contents

Table 9. Orientite and ruizite: electrostatic valence balance of cations and anions<sup>†</sup>

ORIENTITE							
Coordinating cations							
Anions	Ca	Mn(1)	Mn(2)	Si(1)	Si(2)	P <sub>0</sub>	Conclusion
0(1)	2/3	2/3	--	--	2/3	1.79	O <sup>2-</sup>
0(2)	2/3	2/3 + 2/3	--	--	2/3	2.29	O <sup>2-</sup>
0(3)	2/3	--	--	2/3	2/3	2.29	O <sup>2-</sup>
*0(4)	2/3 + 2/3	--	--	2/3	--	1.57	O <sup>2-</sup>
0(5)	--	2/3 + 2/3	--	--	--	1.00	OH <sup>-</sup>
0(6)	2/3	--	--	--	--	0.29	H <sub>2</sub> O
A. Composition Ca <sub>2</sub> □(H <sub>2</sub> O) <sub>2</sub> {Mn <sup>3+</sup> (OH) <sub>2</sub> [Si <sub>3</sub> O <sub>10</sub> ]}. O(4) = O <sup>2-</sup>							
B. Composition Ca <sub>2</sub> Mn <sup>2+</sup> (H <sub>2</sub> O) <sub>2</sub> {Mn <sup>3+</sup> (OH) <sub>2</sub> [(SiO <sub>4</sub> ) <sub>2</sub> (OH) <sub>2</sub> ]}. O(4) = OH <sup>-</sup>							
RUIZITE							
Coordinating cations							
Anions	Ca	Mn	Si(1)	Si(2)	P <sub>0</sub>	Conclusion	
0(1)	2/3	2/3	2/3	--	1.79	O <sup>2-</sup>	
0(2)	2/3	2/3 + 2/3	2/3	--	2.29	O <sup>2-</sup>	
0(3)	2/3	--	2/3	2/3	2.29	O <sup>2-</sup>	
*0(4)	2/3	--	--	2/3	1.29	OH <sup>-</sup> O <sub>2</sub> <sup>2-</sup>	
0(5)	--	--	--	2/3 + 2/3	2.00	O <sup>2-</sup>	
0(6)	--	2/3 + 2/3	--	--	1.00	OH <sup>-</sup>	
0(7)	2/3	--	--	--	0.29	H <sub>2</sub> O	
Composition Ca <sub>2</sub> (H <sub>2</sub> O) <sub>2</sub> {Mn <sup>3+</sup> (OH) <sub>2</sub> [Si <sub>4</sub> O <sub>11</sub> (OH) <sub>2</sub> ]}. O(4) = OH <sup>-</sup> O <sub>2</sub> <sup>2-</sup> .							

<sup>†</sup>Entries include Pauling bond strengths obtained by dividing formal charge by coordination number (C.N. for Ca<sup>2+</sup> = 7, Mn<sup>2+</sup> = 6, Mn<sup>3+</sup> = 6, Si<sup>4+</sup> = 4). Since hydrogen atoms were not determined in the structures, "conclusion" was guided by bond strength sum as bond distance deviations were not listed.

of orientite. Earlier studies met with problems accommodating the high water content proposed in chemical analyses. Finally, the hypothesis of Mellini and Merlino (1982) on the proposed structure for orientite and its relation to ardenite is substantiated, bearing in mind that

a single crystal of orientite end-member has yet to be investigated.

Since hydrogen atoms could not be located in this study, we have selected ruizite and orientite, the latter with and without Mn(2), to construct Table 9. From these electrostatic balance calculations, crude suggestions can be made on which oxygens are hydroxylated. In both instances, these involve O(4) which plays a similar role in both structures. It is an apical or terminal silicate oxygen which also bonds to 2Ca + 2Mn(2) or 2Ca + 1Si(1) for orientite, depending on the absence or presence of bonded silicon. In the former case, we elect O(4) = OH<sup>-</sup>, in the latter O(4) = O<sup>2-</sup>. For ruizite, O(4) bonds to 1Ca + 1Si(2) and we have chosen O(4) = 1/2OH<sup>-</sup> + 1/2O<sup>2-</sup> to balance charge.

A twin model was employed to explain the frequent appearance of bermanite crystals that satisfy X-ray extinctions compatible with space group *C222*<sub>1</sub>. Kampf and Moore (1976) refined this structure in space group *P2*<sub>1</sub> on an untwinned crystal recovered only with considerable difficulty. Does orientite enjoy the same kind of relationship? Although there are many subgroups of *Bbmm*, *Pnmm*, the space group found for ardenite by Donnay and Allmann (1968), is one of them. We have constructed a model for space group *Pnmm* based on the *Bbmm* orientation, which admits both Mn(2) and Si(1) in the structure without steric hindrance in Figure 7. It features both [Si(2)Si(1)Si(2)φ<sub>10</sub>] clusters and [Si(2)Mn(2)Si(2)φ<sub>10</sub>] clusters. The cell contents for the two domains could be 4Ca<sub>2</sub>□(H<sub>2</sub>O)<sub>2</sub>{Mn<sup>3+</sup>(OH)<sub>2</sub>[Si<sub>3</sub>O<sub>10</sub>] with O(4) = O<sup>2-</sup> and 4Ca<sub>2</sub>Mn<sup>2+</sup>(H<sub>2</sub>O)<sub>2</sub>{Mn<sup>3+</sup>(OH)<sub>2</sub>[(SiO<sub>4</sub>)<sub>2</sub>(OH)<sub>2</sub>] with O(4) = OH<sup>-</sup> respectively. From this evidence, we suspect our crystal is an intergrowth of both domains and it is not known if pure single-domain crystals exist. Therefore, the *Bbmm* space group for orientite is probably an averaged model. Finally, a related cell formula can be written for ruizite. It is 2Ca<sub>2</sub>(H<sub>2</sub>O)<sub>2</sub>{Mn<sup>3+</sup>(OH)<sub>2</sub> [Si<sub>4</sub>O<sub>11</sub> (OH)<sub>2</sub>] with O(4) = OH<sup>-</sup><sub>1/2</sub> + O<sub>2</sub><sup>2-</sup>. The O(5) position at (0 0 1/2) in ruizite possesses a *U*<sub>22</sub> parameter which is about one

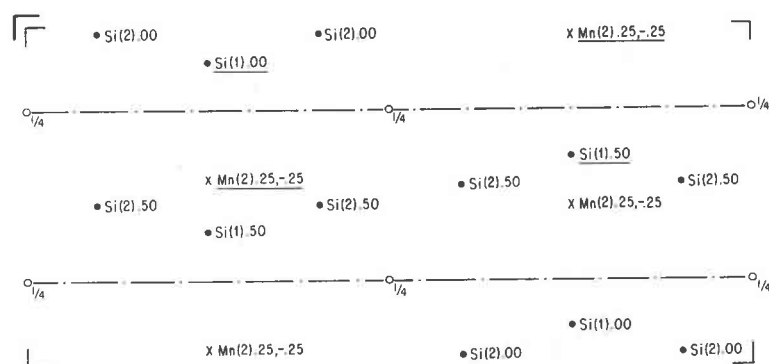


Fig. 7. The Si(1), Si(2) and Mn(2) atoms in orientite projected down the c-axis of the unit cell. The Si positions are denoted by dots and Mn by crosses. A possible site population scheme which is sterically permissible is underlined and involves Si(1) and Mn(2). The subgroup which obtains is *Pnmm*, some of whose symmetry elements are shown.

order of magnitude larger than for the other oxygens, again suggesting disorder.

In all these structures, the fundamental building block  $[\text{Mn}_2^{3+} \square (\text{OH})_2 (\text{TO}_4)_2]$  does not seem to be disturbed, but the difficulties arise in the interlayer material. Therefore, we suspect that the concept of the fundamental building block is a key to relating these structures and that problems of domain structure, twinning and disorder of anionic units occur within the interlayer region. Of all three structure types, not one refined as anticipated for such compounds of intermediate atomic number and we suspect each of them involves some degree of disorder.

#### Acknowledgments

Messrs. Russell P. MacFall and Carlton W. Gutman were especially helpful in rounding up more specimens from the dumps of the Lake Manganese area. P.B.M. acknowledges support from NSF grant EAR81-21193 and J.S. appreciates support from the Ministry of Education, People's Republic of China.

#### References

- Allmann, R. and Donnay, G. (1973) The crystal structure of julgoldite. *Mineralogical Magazine*, 39, 271–281.
- Britton, D. and Dunitz, J. D. (1973) A complete catalogue of polyhedra with eight or fewer vertices. *Acta Crystallographica*, A29, 362–371.
- Burnham, C. W. (1966) Computation of absorption corrections, and the significance of the end effect. *American Mineralogist*, 51, 159–167.
- Cromer, D. T. and Mann, J. B. (1968) X-ray scattering factors computed from numerical Hartree-Fock wave-functions. *Acta Crystallographica*, A24, 321–324.
- Donnay, G. and Allmann, R. (1968)  $\text{Si}_3\text{O}_{10}$  groups in the crystal structure of ardennite. *Acta Crystallographica*, B24, 845–855.
- Galli, E. and Alberti, A. (1969) On the crystal structure of pumpellyite. *Acta Crystallographica*, B25, 2276–2281.
- Gottardi, G. (1965) Die Kristallstruktur von Pumpellyit. *Tschermaks Mineralogische und Petrographische Mitteilungen*, 10, 115–119.
- Harrison, F. W. and Brindley, G. W. (1957) The crystal structure of chloritoid. *Acta Crystallographica*, 10, 77–82.
- Ibers, J. A. and Hamilton, W. C. (1974) *International Tables for X-ray Crystallography*, 4, The Kynoch Press, Birmingham, England, 99–100.
- Kampf, A. R. and Moore, P. B. (1976) The crystal structure of bermanite, a hydrated manganese phosphate. *American Mineralogist*, 61, 1241–1248.
- Mellini, M. and Merlino, S. (1982) Order-disorder in sursassite. *Abstracts of Papers, 13th General Meeting, IMA '82 (Varna, Bulgaria)*, p. 373.
- Moore, P. B. (1981) Complex crystal structures related to glaserite,  $\text{K}_3\text{Na}(\text{SO}_4)_2$ : evidence for very dense packings among oxysalts. *Bulletin de la Société française de Minéralogie et de Cristallographie*, 104, 536–547.
- Moore, P. B. Ito, J. and Steele, I. M. (1979) MacFallite and orientite: calcium manganese (III) silicates from upper Michigan. *Mineralogical Magazine*, 43, 325–331.
- Rumanova, I. M. and Skipetrova, T. I. (1959) The crystal structure of lawsonite. *Doklady Akademia Nauk S.S.S.R.*, 124, 324–327.
- Sun, M.-S. and Weber, R. H. (1958) Santafeite, a new hydrated vanadate from New Mexico. *American Mineralogist*, 43, 677–687.
- Williams, S. A. and Duggan, M. (1977) Ruizite, a new silicate mineral from Christmas, Arizona. *Mineralogical Magazine*, 41, 429–432.

*Manuscript received, May 12, 1983;  
accepted for publication, August 22, 1984.*

Table 6a. Ruizite: anisotropic thermal vibration parameters.<sup>†</sup>

Atom	$U_{11}$	$U_{22}$	$U_{33}$	$U_{12}$	$U_{13}$	$U_{23}$
Mn	8.4(4)	0.1(4)	7.5(4)	0.8(3)	2.5(3)	0.0(3)
Ca	15.7(6)	6.0(5)	10.9(6)	0	2.8(5)	0
Si(1)	7.5(7)	1.9(7)	8.1(7)	0	1.0(6)	0
0(1)	13.9(15)	2.6(13)	12.2(15)	-2.7(11)	5.1(12)	-2.5(11)
0(2)	14.1(21)	3.4(18)	10.1(20)	0	0.2(17)	0
0(3)	17.3(23)	6.9(20)	6.2(19)	0	3.7(17)	0
Si(2)	10.8(8)	12.3(9)	8.1(8)	0	0.8(6)	0
0(4)	67.3(36)	17.3(22)	33.9(26)	-26.3(24)	-31.1(25)	15.4(20)
0(5)	19.4(42)	119.7(65)	17.2(41)	0	7.8(36)	0
0(6)	8.3(19)	4.0(18)	12.1(20)	0	1.4(16)	0
0(7)	17.0(26)	22.0(30)	33.2(33)	0	5.7(24)	0

<sup>†</sup>Coefficients in the expression  $\exp[-U_{11}h^2 + U_{22}k^2 + U_{33}l^2 + 2U_{12}hk + 2U_{13}hl + 2U_{23}kl]$ . Estimated standard errors refer to the last digit. The coefficients are each  $\times 10^3$ .

Table 6b. MacFallite: anisotropic thermal vibration parameters.<sup>†</sup>

Atom	U <sub>11</sub>	U <sub>22</sub>	U <sub>33</sub>	U <sub>12</sub>	U <sub>13</sub>	U <sub>23</sub>
Mn(1)	3.7(3)	17.8(6)	4.6(4)	0.0(4)	1.0(3)	-0.1(4)
Mn(2)	5.2(3)	23.3(5)	5.9(3)	-0.2(4)	1.7(2)	0.4(4)
Mn(3)	5.3(3)	21.2(5)	6.1(3)	-0.2(4)	1.6(2)	0.1(4)
Ca(1)	6.4(4)	23.6(7)	9.9(5)	0	3.1(4)	0
Ca(2)	6.0(4)	26.5(8)	8.6(5)	0	1.5(4)	0
Si(1)	3.1(5)	20.5(10)	4.0(6)	0	1.0(4)	0
O(1)	3.0(11)	22.1(25)	5.5(16)	0	1.3(11)	0
O(2)	3.7(13)	36.6(40)	4.3(15)	0	1.7(12)	0
O(6)	3.7(8)	23.0(21)	6.5(10)	0.5(10)	1.2(8)	-0.9(12)
Si(2)	3.6(5)	18.3(9)	4.5(6)	0	1.5(4)	0
O(3)	4.1(12)	26.7(29)	4.2(14)	0	2.0(11)	0
O(4)	3.4(11)	24.9(27)	4.2(14)	0	0.7(10)	0
O(7)	4.4(8)	22.9(21)	5.7(10)	0.0(11)	1.6(8)	-0.8(12)
Si(3)	4.2(5)	18.6(9)	4.4(6)	0	1.9(4)	0
O(5)	2.6(11)	22.0(24)	6.0(16)	0	1.1(11)	0
O(8)	4.9(7)	20.6(16)	5.4(9)	-0.9(12)	2.1(7)	-0.9(12)
OH(1)	5.6(14)	21.9(25)	5.1(15)	0	2.4(12)	0
OH(2)	4.2(13)	23.8(27)	4.1(14)	0	0.5(11)	0
OH(3)	4.7(14)	30.2(34)	3.6(15)	0	-0.3(12)	0

<sup>†</sup>Coefficients in the expression  $\exp[-U_{11}h^2 + U_{22}k^2 + U_{33}l^2 + 2U_{12}hk + 2U_{13}hl + 2U_{23}kl]$ . Estimated standard errors refer to the last digit. The coefficients are each  $\times 10^3$ .

Table 6c. Orientite: anisotropic thermal vibration parameters.<sup>†</sup>

Atom	$U_{11}$	$U_{22}$	$U_{33}$	$U_{12}$	$U_{13}$	$U_{23}$
Mn(1)	30.0(17)	5.5(3)	53.5(34)	0.1(7)	-0.0(25)	-0.4(8)
Mn(2)	138.6(99)	19.1(16)	230.8(157)	0	13.5(110)	0
Ca	87.1(38)	5.3(5)	71.3(51)	1.7(10)	0	0
Si(1)	93.4(97)	10.4(12)	145.0(139)	0	0	0
O(3)	83.5(142)	4.2(16)	83.5(199)	3.4(37)	0	0
O(4)	52.0(104)	6.3(16)	107.7(218)	0	-0.5(130)	0
Si(2)	37.3(41)	4.3(6)	60.5(69)	0.6(11)	0	0
O(1)	32.7(69)	7.6(12)	88.6(142)	1.8(21)	6.6(76)	-2.1(30)
O(2)	33.3(104)	10.4(20)	68.1(185)	0.4(34)	0	0
O(5)	37.4(111)	7.8(19)	95.0(197)	-0.6(25)	0	0
O(6)	127.7(207)	14.5(27)	210.0(346)	-6.1(61)	0	0

<sup>†</sup>Coefficients in the expression  $\exp[-U_{11}h^2 + U_{22}k^2 + U_{33}l^2 + 2U_{12}hk + 2U_{13}hl + 2U_{23}kl]$ . Estimated standard errors refer to the last digit. The coefficients are each  $\times 10^4$ .